HORMONE RESEARCH IN PÆDIATRICS

Horm Res Paediatr 2010;73:477–481
DOI: 10.1159/000313373

Received: September 7, 2009
Accepted: November 11, 2009
Published online: April 15, 2010

Hypothalamic Dysfunction in a Female with Isolated Hypogonadotropic Hypogonadism and Compound Heterozygous *TACR3* Mutations and Clinical Manifestation in Her Heterozygous Mother

Maki Fukami[a] Tetsuo Maruyama[b] Sumito Dateki[a] Naoko Sato[a]
Yasunori Yoshimura[b] Tsutomu Ogata[a]

[a]Department of Endocrinology and Metabolism, National Research Institute for Child Health and Development, and
[b]Department of Obstetrics and Gynecology, Keio University School of Medicine, Tokyo, Japan

Established Facts

- *TAC3* and *TACR3* have recently been shown to be causative genes for an autosomal recessive form of isolated hypogonadotropic hypogonadism (IHH).

Novel Insights

- Hypothalamic dysfunction may be the primary cause for IHH in patients with biallelic *TACR3* mutations.
- Clinical phenotype may be exhibited by females with heterozygous *TACR3* mutations.
- *TAC3* and *TACR3* mutations remain rare in patients with IHH.

Key Words
Heterozygous manifestation · Hypogonadotropic hypogonadism · Hypothalamus · *TACR3* mutation

Abstract
Background/Aims: *TAC3* and *TACR3* have recently been shown to be causative genes for an autosomal recessive form of isolated hypogonadotropic hypogonadism (IHH). Here, we report a Japanese female with IHH and compound heterozygous *TACR3* mutations and her heterozygous parents, and discuss the primary lesion for IHH and clinical findings. ***Case Report:*** This female was identified through mutation analysis of *TAC3* and *TACR3* in 57 patients with IHH. At 24 years of age, an initial standard GnRH test showed poor gonadotropin response (LH <0.2–0.6 IU/l), whereas the second GnRH test performed after GnRH priming (100 μg i.m. for 5

This work was supported by grants from the Ministry of Health, Labor, and Welfare, and the Ministry of Education, Culture, Sports, Science, and Technology.

KARGER
Fax +41 61 306 12 34
E-Mail karger@karger.ch
www.karger.com

1663–2818/10/0736–0477$26.00/0

Accessible online at:
www.karger.com/hrp

Tsutomu Ogata
Department of Endocrinology and Metabolism
National Research Institute for Child Health and Development
2-10-1 Ohkura, Setagaya, Tokyo 157-8535 (Japan)
Tel. +81 3 5494 7025, Fax +81 3 5494 7026, E-Mail tomogata@nch.go.jp

consecutive days) revealed ameliorated gonadotropin responses (LH 0.3–6.4 IU/l; FSH 2.2–9.6 IU/l). The mother exhibited several features suggestive of mild IHH, whereas the father showed an apparently normal phenotype. ***Results:*** She had a paternally derived nonsense mutation at exon 1 (Y145X) and a maternally inherited single nucleotide (G) deletion from the conserved 'GT' splice donor site of intron 1 (IVS1+1delG). ***Conclusions:*** The results suggest hypothalamic dysfunction as the primary cause for IHH in patients with biallelic *TACR3* mutations and clinical manifestation in heterozygous females, together with the rarity of *TAC3* and *TACR3* mutations in patients with IHH.

Introduction

Isolated hypogonadotropic hypogonadism (IHH) is a genetically heterogeneous condition that lacks other pituitary hormone deficiency [1]. Recently, Topaloglu et al. [2] and Guran et al. [3] have reported homozygous *TAC3* or *TACR3* missense mutations in 11 patients with IHH from 5 Turkish or Kurdish families. TAC3 belongs to an evolutionally conserved neuropeptide family, and TACR3 belongs to a G-protein-coupled receptor family [4]. Topaloglu et al. [2] and Guran et al. [3] also performed functional studies using an intracellular calcium flux system, successfully revealing markedly attenuated activities of the TAC3 and TACR3 mutant proteins. These data provide the first evidence of genetic defects in TAC3/TACR3 signaling being involved in an autosomal recessive form of IHH.

However, there is no other report of *TAC3* or *TACR3* mutations, and further studies are necessary to define the underlying factor(s) for IHH and clinical findings in *TAC3* or *TACR3* mutations. Here, we report a female with IHH and *TACR3* mutations, and discuss the primary cause for IHH and the clinical phenotypes of the patient and her heterozygous parents.

Methods

Mutation Analysis

This study was approved by the Institutional Review Board Committees at the National Center for Child Health and Development and Keio University School of Medicine. After obtaining written informed consent, leukocyte genomic DNA samples from 57 Japanese cases with IHH (38 with 46,XY and 19 with 46,XX) were PCR-amplified with the previously reported primers [2], and subjected to direct sequencing on a CEQ 8000 autosequencer (Beckman Coulter, Fullerton, Calif., USA). To confirm a heterozygous mutation, the corresponding PCR products were subcloned with a TOPO TA Cloning Kit (Invitrogen, Carlsbad, Calif., USA), and the two alleles were sequenced separately.

Prediction of Aberrant Splicing and Nonsense-Mediated mRNA Decay

We utilized the splice site prediction program at the Berkeley Drosophila Genome Project (http://www.fruitfly.org/seq_tools/splice.html) to predict aberrant splicing. On the basis of the previous report [5], we also analyzed whether identified mutations could be subject to nonsense-mediated mRNA decay (NMD) that functions as an mRNA surveillance mechanism to prevent the formation of aberrant proteins.

PCR-Based cDNA Screening for TACR3

Human cDNA samples from control subjects were prepared by RT-PCR or purchased from Clontech (Palo Alto, Calif., USA). PCR amplification was performed for *TACR3* with primers for exon 1 (5′-TTGTGAACCTGGCTTTCTCC-3′) and exon 3 (5′-GGATTTCTCCTCCCCAGAGA-3′), as well as for *GAPDH* utilized as an internal control with primers for the boundary of exons 2/3 (5′-TCGGAGTCAACGGATTTGGTCG-3′) and the boundary of exons 4/5 (5′-TTGGAGGGATCTCGCTCCTG-3′).

Results

Mutation Analysis

Mutation analysis identified two heterozygous mutations of *TACR3* in a female patient, i.e. a nonsense mutation at exon 1 (Y145X) and a single nucleotide (G) deletion from the conserved 'GT' splice donor site of intron 1 (IVS1+1delG; fig. 1A, B). The father was heterozygous for Y145X, and the mother was heterozygous for IVS1+1delG. No demonstrable mutation was detected for *TAC3* in this patient and for *TAC3* and *TACR3* in the remaining 56 cases.

Prediction of Aberrant Splicing and NMD

The IVS1+1delG mutation was predicted to add a 1,153-bp intronic sequence to exon 1 and to cause aberrant splice formation between the added sequence and the normal splice acceptor site of exon 2 (fig. 1C). Furthermore, because of the presence of a stop codon on the added intronic sequence, the IVS1+1delG mutation was predicted to cause a premature termination at the 210th codon. Thus, both IVS1+1delG and Y145X satisfied the conditions for the occurrence of NMD.

PCR-Based cDNA Screening for TACR3

TACR3 expression was clearly identified in the hypothalamus and the pituitary as well as in the whole brain, the ovary, the placenta, and the fetal kidney, but not detected in the testis and leukocytes (fig. 2).

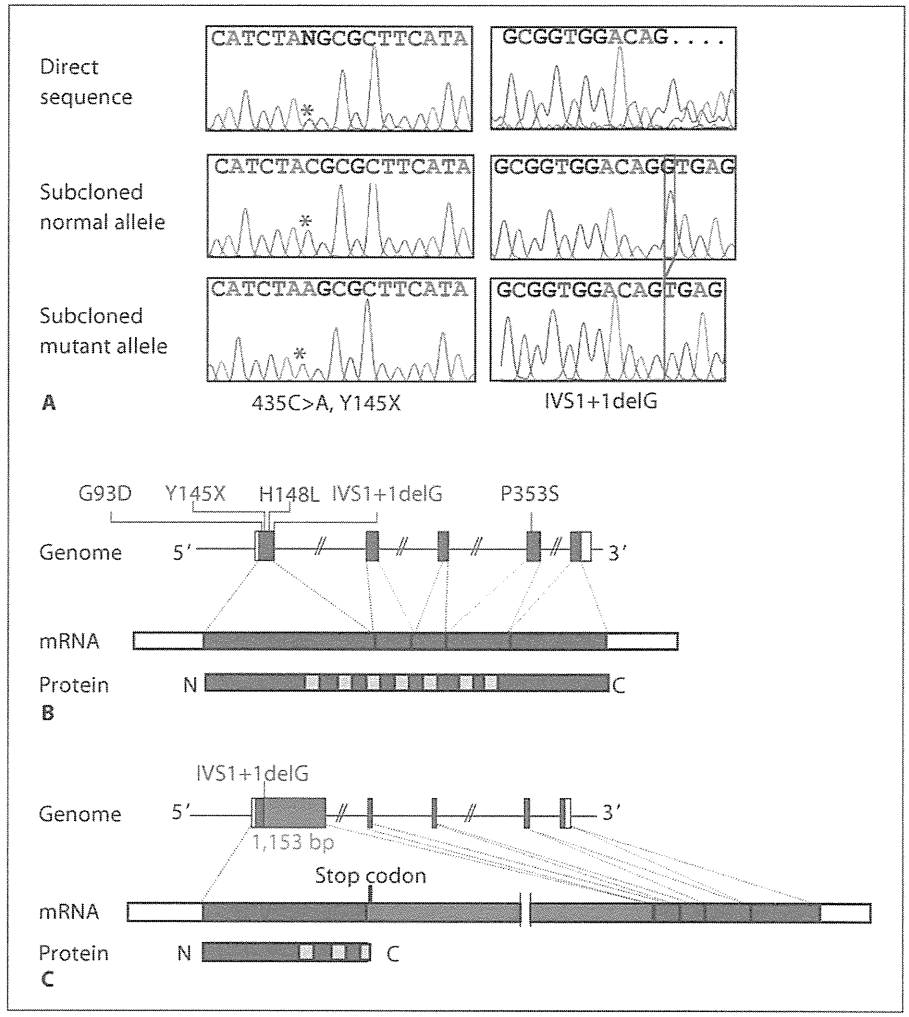

Fig. 1. *TACR3* mutations of the female Japanese patient. **A** Electrochromatograms showing 435C>A (Y145X; indicated by asterisks) and IVS1+1delG (highlighted by red lines). The mutation was indicated by direct sequencing, and confirmed by the subsequently performed sequencing of the subcloned normal and mutant alleles. **B** Schematic presentation of the positions of the mutations. The gray and white boxes on genomic DNA (Genome) and mRNA indicate the coding regions and the untranslated regions on exons 1–5. TACR3 protein (Protein) harbors 7 transmembrane domains (yellow boxes). The mutations identified in the Japanese patient are shown in red, and those reported by Topaloglu et al. [2] and Guran et al. [3] are shown in blue. **C** Predicted consequences of the IVS1+1delG mutation. In silico analysis indicates that IVS1+1delG causes addition of 1,153-bp intronic sequences (green box) to exon 1 and an aberrant splice formation between the added sequence and the normal splice acceptor site of exon 2. The transcribed intronic sequence (green box) harbors a stop codon on its very proximal 5′ region.

Case Report

This Japanese female patient was born as the sole child to nonconsanguineous parents at 42 weeks of gestation after an uncomplicated pregnancy and delivery. Her postnatal growth and development were normal until pubertal age. At 19 years of age, she was seen at a local clinic because of primary amenorrhea. She exhibited poor pubertal development (breast, Tanner stage 1; pubic hair, stage 2), with low basal gonadotropin and estradiol values (table 1). Thus, she received cyclic estrogen and progesterone therapy, and showed periodic withdrawal bleeding. She showed markedly high educational achievement at a university.

At 24 years of age, she was referred to us for further investigations. She measured 163 cm (+0.7 SD) and weighed 48.5 kg (–0.6 SD). Her breast development was at Tanner stage 3–4, and her pubic hair at stage 4. Magnetic resonance imaging delineated normal pituitary structure. Basal blood hormone values measured at 4 weeks after discontinuation of the hormone replacement therapy were consistent with IHH (table 1). Furthermore, while an initial standard GnRH test showed a poor gonadotropin response, the second-time GnRH test performed after GnRH priming (100 μg i.m. for 5 consecutive days) revealed obviously ameliorated gonadotropin responses (table 1).

The 58-year-old mother had menarche at 14.6 years of age (the menarchial age of Japanese females is 9.75–14.75 years). Subsequently, she had regular but long (~45 days) menstrual cycles with occasionally slight intermenstrual bleeding. She had no signs of androgen excess such as hirsutism. She married at 25 years of age, and failed to conceive for 3 years despite an ordinary conjugal life. Basal body temperature records indicated frequent, though not invariable, occurrence of monophasic cycles. Thus, she was treated with chlomiphene citrate by a local medical doctor, and became pregnant at the second cycle of this therapy. Polycystic ovary was excluded by repeatedly performed ultrasound studies during pregnancy. Her menses became irregular from ~45 years of age and ceased at 56 years of age (the menopausal age of Japanese females is 45–56 years). She was otherwise healthy with normal stature (150 cm, –0.5 SD for her age) and intelligence. The 59-year-old father was clinically normal with normal stature (168 cm, +0.9 SD for his age) and intelligence. Allegedly, he had an age-appropriate pubertal development and started shaving at 16 years of age.

Table 1. Endocrine data of the mutation-positive Japanese female

Hormone	Stimulus	Patient		Reference values[1]	
		basal	peak	basal	peak
Examinations at 19 years of age					
LH, mIU/ml		0.4		1.1–4.5	
FSH, mIU/ml		1.7		2.0–6.0	
Estradiol, pg/ml		<4.0		11–82	
Examinations at 24 years of age					
LH, mIU/ml	GnRH[2, 3]	<0.2	0.6	1.1–4.5	2.0–9.2
LH, mIU/ml	GnRH (after priming)[2, 4]	0.3	6.4	1.1–4.5	2.0–9.2[5]
FSH, mIU/ml	GnRH (after priming)[2, 4]	2.2	9.6	2.0–6.0	4.5–12.0[5]
Estradiol, pg/ml		15		11–82	
Prolactin, ng/ml		12.6		2.4–18.7	
TSH, mIU/l		0.75		0.30–4.50	
GH, ng/ml		8.3		<0.1–10.0	
ACTH, pg/ml		8.0		7–56	
AMH, ng/ml		3.4		0.1–7.4	

[1] Reference values in age-matched Japanese females.
[2] Hormone replacement therapy was discontinued for 4 weeks before GnRH tests.
[3] GnRH 100-μg bolus i.v. and blood sampling at 0, 30, 60, 90, and 120 min; FSH was not measured.
[4] GnRH 100-μg bolus i.v. after priming with GnRH 100 μg i.m. for 5 consecutive days.
[5] Reference peak values in a standard GnRH test; there are no reference data after GnRH priming.

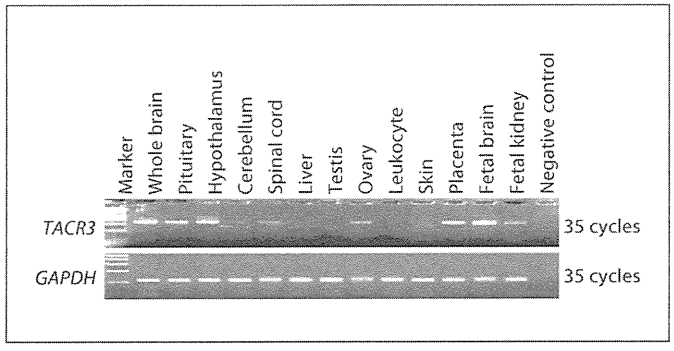

Fig. 2. PCR-based human cDNA screening for *TACR3*. *GAPDH* = Glyceraldehyde-3-phosphate dehydrogenase.

Discussion

This patient had compound heterozygous mutations of *TACR3*. In this regard, both IVS1+1delG and Y145X were predicted as a pathologic mutation missing most of the transmembrane domains. Furthermore, although mRNA was not studied because of absent *TACR3* expression in available leukocytes, both Y145X and IVS1+1delG were predicted to undergo NMD. Thus, the results provide further support for *TACR3* mutations being involved in IHH. Furthermore, the results of the 57 cases suggest the rarity of *TAC3* and *TACR3* mutations in IHH (none for *TAC3* and 1.8% for *TACR3*).

In this patient, it is notable that gonadotropin responses to GnRH stimulation were ameliorated after GnRH priming. This may suggest that the primary lesion for IHH resides in the hypothalamus rather than in the pituitary. Indeed, TACR3 protein is strongly expressed in the human hypothalamus (fig. 2) [6]. Furthermore, rodent Tacr3, Kiss1r (Gpr54), and Gnrh1 proteins are clearly expressed in the median eminence that regulates pulsatile GnRH secretion [7, 8], and human TAC3, KISS1, and ESR1 proteins are co-expressed in the infundibular nucleus that modulates estrogen feedback for gonadotropin secretion [9, 10]. In addition, hypertrophy of TAC3-positive neurons and increased *TAC3* expression have been observed in the hypothalamus of postmenopausal females with hypoestrinism [9]. These data suggest that a molecular network involving TAC3/TACR3, KISS1/KISS1R, and estrogen/ESR1 may underlie the regulation of GnRH secretion in the hypothalamus.

The heterozygous mother exhibited several clinical features suggestive of mild IHH [11]. While such manifestations are apparently absent from the previously re-

ported females heterozygous for *TACR3* missense mutations (G93D, P353S, and H148L) [2, 3], this may be due to the residual activity being retained by the missense mutations but not by the splice donor site mutation of the mother, or to the ethnic difference. Similarly, while the heterozygous father of this patient apparently lacked discernible clinical features, this may be due to sex dimorphism that GnRH secretion remains fairly constant in males and shows dynamic change with menstrual cycles in females [11, 12].

In this study, it appears worthwhile to point out that *TACR3* was clearly expressed in the ovary, but not in the testis. Although the role of *TACR3* in ovarian tissue has not been well studied, a possible involvement of *TACR3* in the development of the corpus luteum has been suggested [13]. Thus, *TACR3* mutations may also have exerted a direct impact on the ovarian function in this patient, independent of gonadotropin deficiency. In addition, the gonadal expression pattern of *TACR3* may be relevant to the phenotypic difference between the mother and father.

In summary, the present study suggests a probable hypothalamic dysfunction in patients with biallelic *TACR3* mutations and heterozygous manifestation in females, together with the rarity of *TAC3* and *TACR3* mutations in patients with IHH. Further studies will help to clarify the clinical and molecular characteristics in *TACR3* mutations.

References

1 Achermann JC, Hughes IA: Disorders of sex development; in Kronenberg HM, Melmed M, Polonsky KS, Larsen PR (eds): Williams Textbook of Endocrinology, ed 11. Philadelphia, Saunders, 2008, pp 783–848.

2 Topaloglu AK, Reimann F, Guclu M, Yalin AS, Kotan LD, Porter KM, Serin A, Mungan NO, Cook JR, Ozbek MN, Imamoglu S, Akalin NS, Yuksel B, O'Rahilly S, Semple RK: TAC3 and TACR3 mutations in familial hypogonadotropic hypogonadism reveal a key role for neurokinin B in the central control of reproduction. Nat Genet 2009;41:354–358.

3 Guran T, Tolhurst G, Bereket A, Rocha N, Porter K, Turan S, Gribble FM, Kotan LD, Akcay T, Atay Z, Canan H, Serin A, O'Rahilly S, Reimann F, Semple RK, Topaloglu AK: Hypogonadotropic hypogonadism due to a novel missense mutation in the first extracellular loop of the neurokinin B receptor. J Clin Endocrinol Metab 2009;94:3633–3639.

4 Almeida TA, Rojo J, Nieto PM, Pinto FM, Hernandez M, Martín JD, Candenas ML: Tachykinins and tachykinin receptors: structure and activity relationships. Curr Med Chem 2004;11:2045–2081.

5 Kuzmiak HA, Maquat LE: Applying nonsense-mediated mRNA decay research to the clinic: progress and challenges. Trends Mol Med 2006;12:306–316.

6 Koutcherov Y, Ashwell KW, Paxinos G: The distribution of the neurokinin B receptor in the human and rat hypothalamus. Neuroreport 2000;11:3127–3131.

7 Krajewski SJ, Anderson MJ, Iles-Shih L, Chen KJ, Urbanski HF, Rance NE: Morphologic evidence that neurokinin B modulates gonadotropin-releasing hormone secretion via neurokinin 3 receptors in the rat median eminence. J Comp Neurol 2005;489:372–386.

8 Messager S, Chatzidaki EE, Ma D, Hendrick AG, Zahn D, Dixon J, Thresher RR, Malinge I, Lomet D, Carlton MB, Colledge WH, Caraty A, Aparicio SA: Kisspeptin directly stimulates gonadotropin-releasing hormone release via G protein-coupled receptor 54. Proc Natl Acad Sci USA 2005;102:1761–1766.

9 Rance NE: Menopause and the human hypothalamus: evidence for the role of kisspeptin/neurokinin B neurons in the regulation of estrogen negative feedback. Peptides 2009;30:111–122.

10 Rometo AM, Krajewski SJ, Voytko ML, Rance NE: Hypertrophy and increased kisspeptin gene expression in the hypothalamic infundibular nucleus of postmenopausal women and ovariectomized monkeys. J Clin Endocrinol Metab 2007;92:2744–2750.

11 Bulun SE, Adashi EY: The physiology and pathology of the female reproductive axis; in Kronenberg HM, Melmed M, Polonsky KS, Larsen PR (eds): Williams Textbook of Endocrinology, ed 11. Philadelphia, Saunders. 2008, pp 541–614.

12 Goh HH, Ratnam SS: The LH surge in humans: its mechanism and sex difference. Gynecol Endocrinol 1988;2:165–182.

13 Brylla E, Aust G, Geyer M, Uckermann O, Löffler S, Spanel-Borowski K: Coexpression of preprotachykinin A and B transcripts in the bovine corpus luteum and evidence for functional neurokinin receptor activity in luteal endothelial cells and ovarian macrophages. Regul Pept 2005;125:125–133.

Endocrine Journal 2010, 57 (2), 171-174

Diabetes Mellitus in a Japanese Girl with HDR Syndrome and *GATA3* Mutation

KOJI MUROYA[1),2)], TAKAHIRO MOCHIZUKI[3)], MAKI FUKAMI[1)], MANAMI ISO[1)], KEINOSUKE FUJITA[3)], MITSUO ITAKURA[4)] AND TSUTOMU OGATA[1)]

[1)] *Department of Endocrinology and Metabolism, National Research Institute for Child Health and Development, Tokyo, Japan*
[2)] *Department of Endocrinology and Metabolism, Kanagawa Children's Medical Center, Yokohama, Japan*
[3)] *Department of Pediatrics, Children's Medical Center, Osaka City General Hospital, Osaka, Japan*
[4)] *Institute for Genome Research, Tokushima University, Tokushima, Japan*

Abstract. We report on a Japanese girl with HDR (*h*ypoparathyroidism, sensorineural *d*eafness, and *r*enal dysplasia) syndrome who developed diabetes mellitus (DM) at three years of age (blood glucose 713 mg/dL, HbA_{1c} 8.0%) in the absence of anti-glutamic acid decarboxylase autoantibodies. Mutation analysis revealed a *de novo* heterozygous two base pair deletion at exon 6 of the *GATA3* gene (c.1200_1201delCA; p.H400fsX506). *GATA3* expression was identified by PCR amplification for human pancreas cDNA, and mouse *Gata3* was weekly but unequivocally expressed in pancreatic β cells. The results, in conjunction with the previous findings indicating the critical role of *GATA3* in lymphocyte function, suggest that *GATA3* haploinsufficiency may affect the function of β cells and/or lymphocytes, leading to the development of DM in relatively exceptional patients with high susceptibility to DM.

Key words: Diabetes mellitus, Expression, *GATA3*, HDR syndrome

HDR (*h*ypoparathyroidism, sensorineural *d*eafness, and *r*enal dysplasia) syndrome is an autosomal dominant disorder first reported by Bilous *et al.* [1]. This condition is primarily caused by haploinsufficiency of *GATA3* on chromosome 10p15, although a *GATA3* mutation has not been identified in several patients with HDR syndrome-compatible clinical features [2, 3]. *GATA3* consists of six exons, and encodes a transcription factor with two transactivation domains and two zinc finger domains [2]. *GATA3* is expressed in the developing parathyroid glands, inner ears, and kidneys, together with thymus and central nervous system [4, 5]. While several non-triad features such as pyloric stenosis, ventricular septal defect, polycystic ovary, abnormal Müllerian duct structures, and hemimegalencephaly have been described in several patients with *GATA3* mutations [3, 6–8], there is no report documenting diabetes mellitus (DM) in this condition.

Here, we report a patient with DM and a *GATA3* mutation, and discuss a potential relationship between DM and a *GATA3* mutation.

Received Oct. 26, 2009; Accepted Nov. 19, 2009 as K09E-313
Released online in J-STAGE as advance publication Dec. 1, 2009

Correspondence to: Dr. Tsutomu OGATA, Department of Endocrinology and Metabolism, National Research Institute for Child Health and Development, 2-10-1 Ohkura, Setagaya, Tokyo 157-8535, Japan. E-mail: tomogata@nch.go.jp

Case Report

This Japanese girl was born at 37 weeks of gestation after an uncomplicated pregnancy and delivery. At birth, her length was 43.0 cm (–2.4 SD) and her weight 1.74 kg (–3.1 SD). The non-consanguineous parents and the younger brother were clinically normal.

At 3 months of age, she was admitted to Osaka City Medical Center because of frequent vomiting and irritability. Routine laboratory tests revealed hypocalcemia (7.8 mg/dL) (age- and sex-matched Japanese reference value, 9.8–11.6 mg/dL) and hyperphosphatemia (8.3 mg/dL) (5.1–7.1 mg/dL), and subsequent biochemical studies showed parathyroid hormone (PTH) deficiency (intact PTH, below 5 pg/mL) (10–50 pg/mL). Thus, 1α-(OH) vitamin D therapy was started, successfully normalizing serum calcium and phosphate values. At 12 months of age, since she

responded poorly to sounds, auditory brainstem response was performed, indicating severe sensorineural deafness with hearing levels being 80 dB for the right ear and 100 dB for the left ear (normal range, below 25 dB). Thus, hearing aids were utilized in her daily life.

At 3 years of age, she showed polydipsia, polyuria, and weight loss, and was diagnosed as having DM because of elevated blood glucose (713 mg/dL) (70–110 mg/dL) and HbA_{1c} (8.0%) (4.3–5.8%). Serum insulin was 8.0 μU/mL (1.7–10.4μU/mL) and C-peptide 1.1 ng/mL (0.6–1.8 ng/mL). She was immediately placed on insulin therapy (~0.7 U/kg/day). Urine C-peptide gradually decreased and became undetectable at eight years of age; at that time, she required insulin therapy of 1.08 U/kg/day. Anti-glutamic acid decarboxylase autoantibodies (anti-GAD Abs) were negative throughout the clinical course. At nine years of age, she was found to have elevated blood urea nitrogen (61.3 mg/dL) (7.5–19.3 mg/dL) and creatinine (2.0 mg/dL) (0.4–0.8 mg/dL) at the time of periodical follow-up examinations for DM. Thus, renal echography and scntigraphy were performed, showing right renal aplasia and left renal hypoplasia. Other abdominal visceral organs including the pancreas exhibited apparently normal structures on the ultrasound examinations. Chromosome analysis revealed a 46,XX karyotype in all the 50 lymphocytes examined. On the basis of the above findings, she was diagnosed as having HDR syndrome and DM. At present, she is 12 years old, and shows short stature (–4.5 SD) and some pubertal development (breast, Tanner stage 2). Current insulin dosage is 1.17 U/kg/day, and her DM has been well controlled with HbA1c value being maintained around 6.0%.

Methods

Mutation analysis of GATA3

This study was approved by the Institutional Review Board Committee at National Center for Child Health and Development. After obtaining informed consent, leukocyte genomic DNA samples of the patient and the parents were PCR-amplified for the coding exons 2–6 and their splice sites, and the PCR products were subjected to direct sequencing from both directions on a CEQ 8000 autosequencer (Beckman Coulter, Fullerton, CA). The primer sequences and the PCR conditions were as described previously [2, 3]. To confirm a heterozygous mutation, the corresponding PCR products were subcloned with a TOPO TA Cloning Kit (Invitrogen, Carlsbad, CA), and normal and mutant alleles were sequenced separately.

PCR amplification of human pancreas cDNA

Human pancreas cDNA was purchased from Clontech (Mountain View, CA), as well as fetal kidney cDNA utilized as a positive control. PCR amplification was performed with 0.5 ng of cDNA samples, using the forward primer for exon 5 (5'–GAATGCCA-ATGGGGACCCTGT–3') and the reverse primer for exon 6 (5'–TTCATGCCTTACAGCTACCCAGA–3').

In situ hybridization (ISH) analysis for the mouse pancreas

Fifteen-week-old female BDF1 mice (Clea Japan, Tokyo) were anesthetized with sodium pentobarbital and fixed by cardiac perfusion with Mildform10N (Wako Pure Chemical Industries, Osaka). Pancreatic tissues were dissected and fixed with the same fixative for 48 hours at room temperature. The tissues were embedded in paraffin, and serial tissue sections were prepared at 5 μm thickness. ISH analysis was performed with BlueMap Kit and Discovery automatic staining modules (Ventana Medical Systems, Tucson, AZ) according to manufacturer's instructions. cDNAs of mouse *Ins-1* (an insulin-like peptide orthologous to human insulin) (nt 653–1117, GenBank accession no. X04725) and *Gata3* (nt 1566–2002, GenBank accession no. NM_008091) were amplified by reverse transcription PCR and subcloned into pCR4Blunt-TOPO (Invitrogen). Sense and antisense digoxigenin-labeled RNA probes were synthesized using T7 or T3 RNA polymerase in the presence of digoxigenin-labeled dUTP following the manufacturer's protocol (Roche Molecular Biochemicals, Indianapolis, IN).

Results

Mutation analysis of GATA3

This patient had a heterozygous two base pair deletion at exon 6 (c.1200_1201delCA) of *GATA3* that is predicted to cause a frameshift at the 400th codon for the histidine and resultant termination at the 506th codon (p.H400fsX506) (Fig. 1). This mutation was absent from the parents.

PCR amplification of human pancreas cDNA

PCR products of 690 bp long were identified in fe-

tal kidney after 25 cycles and in pancreas after 40 cycles (Fig. 2A). This indicated relatively weak *GATA3* expression in the pancreas.

ISH analysis for the mouse pancreas

Anti-sense probes for *Gata3* detected weak but definitive signals in cells with strong *Ins-1* expression (Fig. 2B). This showed specific *Gata3* expression in the mouse pancreatic β cells.

Discussion

This patient had the triad of the HDR syndrome and a heterozygous mutation of *GATA3*. This is consistent with the previous data indicating that *GATA3* mutations are usually identified in patients with two or three of the HDR triad features [9, 10].

The salient feature of this patient is the development of DM. This may be co-incidental, because DM has not been identified in patients with *GATA3* mutations. However, human *GATA3* was identified in the human pancreas cDNA sample, and mouse *Gata3* was weekly but unequivocally expressed in pancreatic β cells. In addition, *GATA3* is known to play an important role in lymphocyte development and function [11, 12]. Thus, *GATA3* haploinsufficiency may affect the function of β cells and/or lymphocytes, leading to the development of DM in relatively exceptional patients with high susceptibility to DM because of other genetic and environmental factors. In this regard, the absence of anti-GAD Abs may argue for possible β cell, rather than lymphocyte, dysfunction [13].

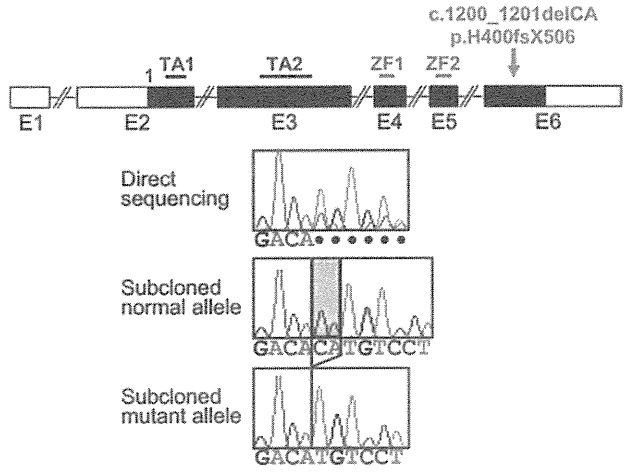

Fig. 1. Mutation analysis of *GATA3*.
Upper diagram: The genomic structure of *GATA3*. The black and white boxes denote the coding and the untranslated regions, respectively. TA1 and TA2 denote two transactivation domains, and ZF1 and ZF2 represent two zinc finger domains.
Lower diagram: The electrochromatograms delineate the c.1200_1201delCA (p.H400fsX506) mutation at exon 6. This mutation has been indicated by the direct sequencing, and confirmed by the subsequently performed sequencing of the subcloned normal and mutant alleles.

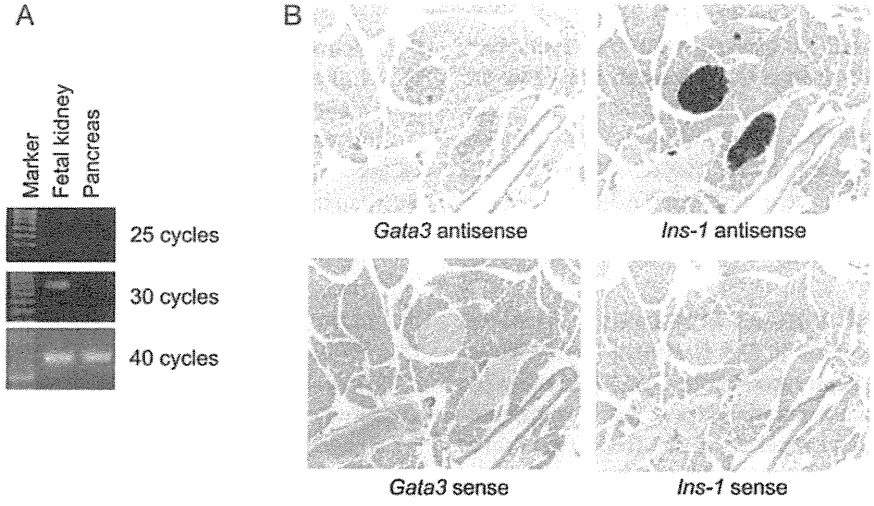

Fig. 2. Expression analyses of *GATA3/Gata3*.
A. PCR-amplification using human cDNA samples. *GATA3* expression is identified after 25 cycles in the fetal kidney, and after 40 cycles in the pancreas.
B. ISH analysis using the mouse pancreas. The antisense probe for *Gata3* detects weak but positive signals in the cells with strong expression of *Ins-1* (β cells). No signals have been identified by the sense probes.

The frameshift mutation resided on the last coding exon 6. Since the position of the mutation satisfies the condition for the escape from nonsense mediated mRNA decay [14], it is possible that an aberrant GATA3 protein is produced, leading to the development of DM due to a dominant negative effect. However, this possibility is unlikely, because previously reported patients with nonsense or frameshift mutations on exon 6 are free from DM [3, 10].

In summary, we observed a patient with a *GATA3* mutation and DM. Further studies will clarify whether *GATA3* mutations can be a risk factor for the development of DM.

Acknowledgements

This work was supported in part by grants for Child Health and Development and for Research on Children and Families from the Ministry of Health, Labor, and Welfare.

References

1. Bilous RW, Murty G, Parkinson DB, Thakker RV, Coulthard MG, Burn J, Mathias D, Kendall-Taylor P (1992) Autosomal dominant familial hypoparathyroidism, sensorineural deafness, and renal dysplasia. *N Engl J Med* 327: 1069–1074.
2. Van Esch H, Groenen P, Nesbit MA, Schuffenhauer S, Lichtner P, Vanderlinden G, Harding B, Beetz R, Bilous RW, Holdaway I, Shaw NJ, Fryns JP, Van de Ven W, Thakker RV, Devriendt K (2000) GATA3 haplo-insufficiency causes human HDR syndrome. *Nature* 406: 419–422.
3. Muroya K, Hasegawa T, Ito Y, Nagai T, Isotani H, Iwata Y, Yamamoto K, Fujimoto S, Seishu S, Fukushima Y, Hasegawa Y, Ogata T (2001) GATA3 abnormalities and the phenotypic spectrum of HDR syndrome. *J Med Genet* 38: 374–380.
4. Labastie MC, Catala M, Gregoire JM, Peault B (1995) The GATA3 gene is expressed during human kidney embryogenesis. *Kidney Int* 47: 1597–1603.
5. Debacker C, Catala M, Labastie MC (1999) Embryonic expression of the human GATA3 gene. *Mech Dev* 85: 183–187.
6. Zahirieh A, Nesbit MA, Ali A, Wang K, He N, Stangou M, Bamichas G, Sombolos K, Thakker RV, Pei Y (2005) Functional analysis of a novel GATA3 mutation in a family with the hypoparathyroidism, deafness, and renal dysplasia syndrome. *J Clin Endocrinol Metab* 90: 2445–2450.
7. Hernández AM, Villamar M, Roselló L, Moreno-Pelayo MA, Moreno F, Del Castillo I (2007) Novel mutation in the gene encoding the GATA3 transcription factor in a Spanish familial case of hypoparathyroidism, deafness, and renal dysplasia (HDR) syndrome with female genital tract malformations. *Am J Med Genet A* 143: 757–762.
8. Adachi M, Tachibana K, Asakura Y, Tsuchiya T (2006) A novel mutation in the GATA3 gene in a family with HDR syndrome (hypoparathyroidism, sensorineural deafness and renal anomaly syndrome). *J Pediatr Endocrinol Metab* 19: 87–92.
9. Nesbit MA, Bowl MR, Harding B, Ali A, Ayala A, Crowe C, Dobbie A, Hampson G, Holdaway I, Levine MA, McWilliams R, Rigden S, Sampson J, Williams AJ, Thakker RV (2004) Characterization of GATA3 mutations in the hypoparathyroidism, deafness, and renal dysplasia (HDR) syndrome. *J Biol Chem* 279: 22624–22634.
10. Ali A, Christie PT, Grigorieva IV, Harding B, Van Esch H, Ahmed SF, Bitner-Glindzicz M, Blind E, Bloch C, Christin P, Clayton P, Gecz J, Gilbert-Dussardier B, Guillen-Navarro E, Hackett A, Halac I, Hendy GN, Lalloo F, Mache CJ, Mughal Z, Ong AC, Rinat C, Shaw N, Smithson SF, Tolmie J, Weill J, Nesbit MA, Thakker RV (2007) Functional characterization of GATA3 mutations causing the hypoparathyroidism-deafness-renal (HDR) dysplasia syndrome: insight into mechanisms of DNA binding by the GATA3 transcription factor. *Hum Mol Genet* 16: 265–275.
11. Labastie MC, Bories D, Chabret C, Grégoire JM, Chrétien S, Roméo PH (1994) Structure and expression of the human GATA3 gene. *Genomics* 21: 1–6.
12. Hendriks RW, Nawijn MC, Engel JD, van Doorninck H, Grosveld F, Karis A (1999) Expression of the transcription factor GATA-3 is required for the development of the earliest T cell progenitors and correlates with stages of cellular proliferation in the thymus. *Eur J Immunol* 29: 1912–1918.
13. Eisenabrth GS, Polonsky KS, Buse JB (2008) Type 1 diabetes mellitus. In: Kronenberg HM, Melmed S, Polonsky KS, Larsen PR (eds). Williams textbook of endocrinology, 11th ed. W.B. Saunders, Philadelphia, pp 1391–1416.
14. Kuzmiak HA, Maquat LE (2006) Applying nonsense-mediated mRNA decay research to the clinic: progress and challenges. *Trends Mol Med* 12: 306–316.

Parthenogenetic chimaerism/mosaicism with a Silver-Russell syndrome-like phenotype

K Yamazawa,[1,2] K Nakabayashi,[3] M Kagami,[1] T Sato,[1] S Saitoh,[4] R Horikawa,[5] N Hizuka,[6] T Ogata[1]

► Additional figures, tables and an appendix are published online only. To view these files, please visit the journal online (http://jmg.bmj.com).

[1]Departments of Endocrinology and Metabolism, National Research Institute for Child Health and Development, Tokyo, Japan
[2]Department of Physiology, Development & Neuroscience, University of Cambridge, Cambridge, UK
[3]Maternal-Fetal Biology, National Research Institute for Child Health and Development, Tokyo, Japan
[4]Department of Pediatrics, Hokkaido University Graduate School of Medicine, Sapporo, Japan
[5]Division of Endocrinology and Metabolism, National Children's Hospital, Tokyo, Japan
[6]Department of Medicine, Institute of Clinical Endocrinology, Tokyo Women's Medical University, Tokyo, Japan

Correspondence to
Dr Tsutomu Ogata, Department of Endocrinology and Metabolism, National Research Institute for Child Health and Development, 2-10-1 Ohkura, Setagaya, Tokyo 157-8535, Japan; tomogata@nch.go.jp

Received 20 March 2010
Revised 6 May 2010
Accepted 8 May 2010
Published Online First 3 August 2010

ABSTRACT

Introduction We report a 34-year-old Japanese female with a Silver-Russell syndrome (SRS)-like phenotype and a mosaic Turner syndrome karyotype (45,X/46,XX).

Methods/Results Molecular studies including methylation analysis of 17 differentially methylated regions (DMRs) on the autosomes and the *XIST*-DMR on the X chromosome and genome-wide microsatellite analysis for 96 autosomal loci and 30 X chromosomal loci revealed that the 46,XX cell lineage was accompanied by maternal uniparental isodisomy for all chromosomes (upid(AC)mat), whereas the 45,X cell lineage was associated with biparentally derived autosomes and a maternally derived X chromosome. The frequency of the 46,XX upid(AC)mat cells was calculated as 84% in leukocytes, 56% in salivary cells, and 18% in buccal epithelial cells.

Discussion The results imply that a parthenogenetic activation took place around the time of fertilisation of a sperm missing a sex chromosome, resulting in the generation of the upid(AC)mat 46,XX cell lineage by endoreplication of one blastomere containing a female pronucleus and the 45,X cell lineage by union of male and female pronuclei. It is likely that the extent of overall (epi)genetic aberrations exceeded the threshold level for the development of SRS phenotype, but not for the occurrence of other imprinting disorders or recessive Mendelian disorders.

Although a mammal with maternal uniparental disomy for all chromosomes (upd(AC)mat) is incompatible with life because of genomic imprinting,[1] a mammal with a upd(AC)mat cell lineage could be viable in the presence of a co-existing normal cell lineage. In the human, Strain *et al*[2] have reported 46,XX peripheral blood cells with maternal uniparental isodisomy for all chromosomes (upid(AC)mat) in a 1.2-year-old phenotypically male patient with aggressive behaviour, hemifacial hypoplasia and normal birth weight. Because of the 46,XX disorders of sex development, detailed molecular studies were performed, revealing the presence of a normal 46,XY cell lineage in a vast majority of skin fibroblasts and a upid(AC)mat 46,XX cell lineage in nearly all blood cells. In addition, although the data are insufficient to draw a definitive conclusion, Horike *et al*[3] have also identified 46,XX peripheral blood cells with possible upd(AC)mat in a phenotypically male patient through methylation analyses for plural differentially methylated regions (DMRs) in 11 patients with Silver–Russell syndrome (SRS)-like phenotype. This patient was found to have a normal 46,XY cell lineage and a triploid 69,XXY cell lineage in skin fibroblasts.

However, such patients with a upd(AC)mat cell lineage remain extremely rare, and there is no report describing a human with such a cell lineage in the absence of a normal cell lineage. Here, we report a female patient with a upid(AC)mat 46,XX cell lineage and a non-upd 45,X cell lineage who was identified through genetic screenings of 103 patients with SRS-like phenotype.

MATERIALS AND METHODS

Case report

This Japanese female patient was conceived naturally and born at 40 weeks of gestation by a normal vaginal delivery. At birth, her length was 44.0 cm (−3.1 SD), her weight 2.1 kg (−2.9 SD) and her occipitofrontal head circumference (OFC) 30.5 cm (−2.3 SD). The parents and the younger brother were clinically normal (the father died from a traffic accident).

At 2 years of age, she was referred to us because of growth failure. Her height was 77.7 cm (−2.5 SD), her weight 8.45 kg (−2.6 SD) and her OFC 43.5 cm (−2.5 SD). Physical examination revealed several SRS-like somatic features such as triangular face, right hemihypoplasia and bilateral fifth finger clinodactyly. She also had developmental retardation, with a developmental quotient of 56. Endocrine studies for short stature were normal as were radiological studies. Cytogenetic analysis using lymphocytes indicated a low-grade mosaic Turner syndrome (TS) karyotype, 45,X[3]/46,XX[47]. Thus, a screening of TS phenotype[4] was performed, detecting horseshoe kidney but no body surface features or cardiovascular lesion. Chromosome analysis was repeated at 6 and 32 years of age using lymphocytes, revealing a 45,X[8]/46,XX[92] karyotype and a 45,X[12]/46,XX[88] karyotype, respectively. On the last examination at 34 years of age, her height was 125.0 cm (−6.2 SD), her weight 37.5 kg (−2.0 SD) and her OFC 51.2 cm (−2.8 SD). She was engaged in a simple work and was able to get on her daily life for herself.

Sample preparation

This study was approved by the Institutional Review Board Committees at National Center for Child health and Development. After obtaining written informed consent, genomic DNA was extracted from leukocytes of the patient, the mother and the brother and from salivary cells, which comprise ~40% of buccal epithelial cells and ~60% of leukocytes,[5] of the patient. Lymphocyte metaphase spreads and leukocyte RNA were also

obtained from the patient. Leukocytes of healthy adults and patients with imprinting disorders were utilised for controls.

Primers and probes

The primers utilised in this study are summarised in supplementary methods and supplementary tables 1–3.

DMR analyses

We first performed bio-combined bisulfite restriction analysis (COBRA)[6] and bisulfite sequencing of the *H19*-DMR (A) on chromosome 11p15.5 by the previously described methods[7] and methylation-sensitive PCR analysis of the *MEST*-DMR (A) on chromosome 7q32.2 by the previously described methods[8] with minor modifications (the methylated and unmethylated allele-specific primers were designed to yield PCR products of different sizes, and the PCR products were visualised on the 2100 Bioanalyzer (Agilent, Santa Clara, California, USA)). This was because hypomethylation (epimutation) of the normally methylated *H19*-DMR of paternal origin and maternal uniparental disomy 7 are known to account for 35–65% and 5–10% of SRS patients, respectively.[9 10] In addition, fluorescence in situ hybridisation (FISH) analysis was performed with a ~84-kb RP5-998N23 probe containing the *H19*-DMR (BACPAC Resources Center, Oakland, California, USA). We also examined multiple other DMRs by bio-COBRA. The ratio of methylated clones (the methylation index) was calculated using peak heights of digested and undigested fragments on the 2100 Bioanalyzer using 2100 expert software.

Genome-wide microsatellite analysis

Microsatellite analysis was performed for 96 autosomal loci and 30 X chromosomal loci. The segment encompassing each locus was PCR-amplified, and the PCR product size was determined on the ABI PRISM 310 autosequencer using GeneScan software (Applied Biosystems, Foster City, California, USA).

PCR analysis for Y chromosomal loci

Standard PCR was performed for six Y chromosomal loci. The PCR products were electrophoresed using the 2100 Bioanalyzer.

Expression analysis

Quantitative real-time reverse transcriptase PCR analysis was performed for three paternally expressed genes (*IGF2*, *SNRPN* and *ZAC1*) and four maternally expressed genes (*H19*, *MEG3*, *PHLDA2* and *CDKN1C*) that are known to be variably (usually weakly) expressed in leukocytes (UniGene, http://www.ncbi.nlm.nih.gov/sites/entrez?db=unigene), using an ABI Prism 7000 Sequence Detection System (Applied Biosystems). *TBP* and *GAPDH* were utilised as internal controls.

RESULTS

DMR analyses

In leukocytes, the bio-COBRA indicated severely hypomethylated *H19*-DMR, and bisulfite sequencing combined with *rs2251375* SNP typing for 30 clones revealed maternal origin of 29 hypomethylated clones and non-maternal (paternal) origin of a single methylated clone in this patient (figure 1A). Thus, the marked hypomethylation of the *H19*-DMR was caused by predominance of maternally derived clones rather than hypomethylation of the *H19*-DMR of paternal origin. FISH analysis for 100 lymphocyte metaphase spreads excluded an apparent deletion of the paternally derived *H19*-DMR or duplication of the maternally derived *H19*-DMR (Supplementary figure 1). Methylation-sensitive PCR amplification for the *MEST*-DMR delineated a major peak for the methylated allele and a minor peak for the unmethylated allele (figure 1B). This also indicated the predominance of maternally derived clones and the co-existence of a minor portion of paternally derived clones. Furthermore, autosomal DMRs invariably exhibited markedly abnormal methylation patterns consistent with predominance of maternally inherited DMRs, whereas the methylation index of the *XIST*-DMR on the X chromosome remained within the female reference range (figure 1C). The abnormal methylation patterns were less obvious in salivary cells (thus, in buccal epithelial cells) than in leukocytes, except for the methylation index for the *XIST*-DMR that mildly exceeded the female reference range (figure 1A–C).

Microsatellite analysis

Major peaks consistent with maternal uniparental isodisomy and minor peaks of non-maternal (paternal) origin were identified for at least one locus on each autosome, with the minor peaks of non-maternal origin being more obvious in salivary cells than in leukocytes (figure 1D and supplementary table 4). Furthermore, the frequency of the upid(AC)mat cells was calculated as 84% in leukocytes, 56% in salivary cells and 18% in epithelial buccal cells, using the area under curves for the maternally and the non-maternally inherited peaks (supplementary note). Such minor peaks of non-maternal origin were not detected for all the 30 X chromosomal loci examined.

PCR analysis for Y chromosomal loci

PCR amplification failed to detect any trace of Y chromosome-specific bands in leukocytes and salivary cells (Supplementary figure 2).

Expression analysis

Expression analysis using control leukocytes indicated that, of the seven examined genes, *SNRPN* expression alone was strong enough to allow for a precise assessment (Supplementary figure 3). *SNRPN* expression was extremely low in this patient (figure 1E).

DISCUSSION

These results imply that this patient had a upid(AC)mat 46,XX cell lineage and a non-upd 45,X cell lineage. Indeed, methylation patterns of the *XIST*-DMR is explained by assuming that the two X chromosomes in the upid(AC)mat cells undergo random X-inactivation and that 45,X cells with the methylated *XIST*-DMR on a single active X chromosome[11] are relatively prevalent in buccal epithelial cells. Furthermore, lack of non-maternally derived minor peaks for microsatellite loci on the X chromosome is explained by assuming that the two X chromosomes in the upid(AC)mat cells and the single X chromosome in the 45,X cells are derived from a common X chromosome of maternal origin, with no paternally derived sex chromosome. It is likely, therefore, that a parthenogenetic activation took place around the time of fertilisation of a sperm missing a sex chromosome, resulting in the generation of the 46,XX cell lineage with upid (AC)mat by endoreplication (the replication of DNA without the subsequent completion of mitosis) of one blastomere containing a female pronucleus and the 45,X cell lineage with biparentally derived autosomes and a maternally derived X chromosome by union of male and female pronuclei (figure 2), although it is also possible that a paternally derived sex chromosome was present in the sperm but was lost from the normal

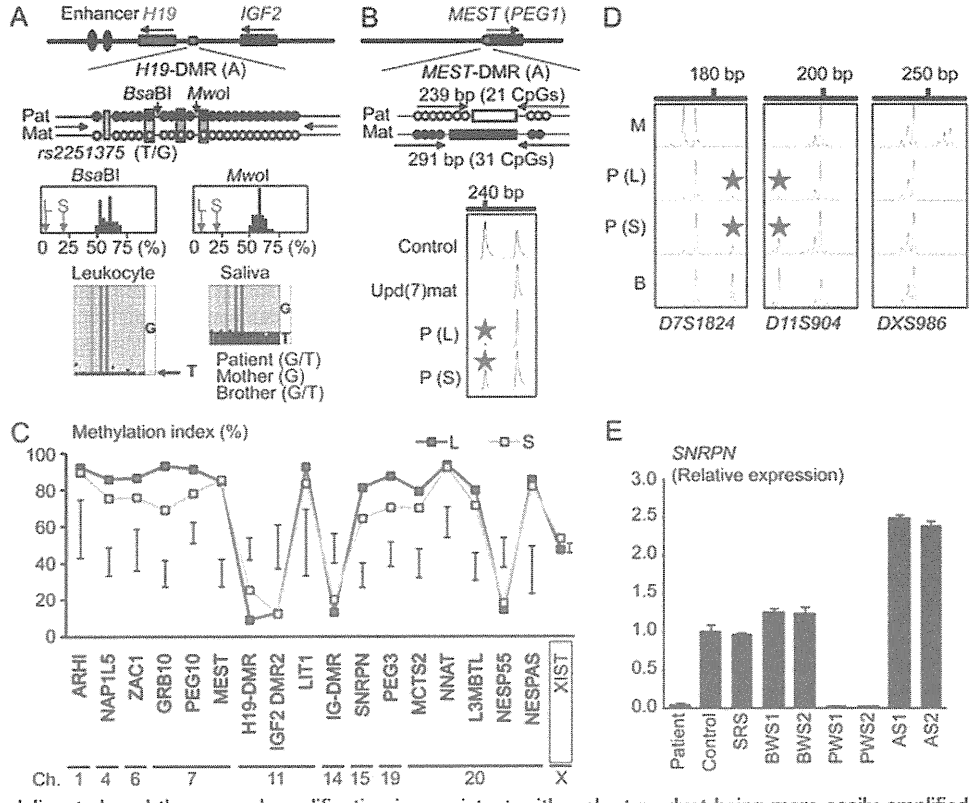

Figure 1 Representative molecular results. Pat, paternally derived allele; Mat, maternally derived allele; P, patient; M, mother; B, brother; L, leukocytes; and S, salivary cells. Filled and open circles in A and B represent methylated and unmethylated cytosine residues at the CpG dinucleotides, respectively. A. Methylation patterns of the *H19*-DMR (A) harbouring 23 CpG dinucleotides and the T/G SNP (*rs2251375*) (a grey box). The PCR products are digested with *Bsa*BI when the cytosine at the sixth CpG dinucleotide (highlighted in yellow) is methylated and with *Mwo*I when the two cytosines at the ninth and the 11th CpG dinucleotides (highlighted in orange) are methylated. For the bio-COBRA data, the black histograms represent the distribution of methylation indices (%) in 50 control participants, and L and S denote the methylation indices for leukocytes and salivary cells of this patient, respectively. For the bisulfite sequencing data, each line indicates a single clone. B. Methylated and unmethylated allele-specific PCR analysis for the *MEST*-DMR (A). In a control participant, the PCR products for methylated and unmethylated alleles are delineated, and the unequal amplification is consistent with a short product being more easily amplified than a long product. In a previously reported patient with upd(7)mat,[8] the methylated allele only is amplified. In this patient, major peaks for the methylated allele and minor peaks for the unmethylated allele (red asterisks) are detected. C. Methylation patterns for the 18 DMRs examined. The DMRs highlighted in blue and pink are methylated after paternal and maternal transmissions, respectively. The black vertical bars indicate the reference data (maximum–minimum) in 20 normal control participants, using leukocyte genomic DNA (for the *XIST*-DMR, 16 female data are shown). D. Representative microsatellite analysis. Minor peaks (red asterisks) have been identified for *D7S1824* and *D11S904* but not for *DXS986* of the patient. Since the peaks for *D7S1824* and *D11S904* are absent in the mother and clearly present in the brother, they are assessed to be of paternal origin. E. Relative expression level (mean ± SD) of *SNRPN* on chromosome 15. The data have been normalised against *TBP*. SRS, an SRS patient with an epimutation (hypomethylation) of the *H19*-DMR; BWS1, a BWS patient with an epimutation (hypermethylation) of the *H19*-DMR; BWS2, a BWS patient with upd(11)pat; PWS1, a PWS patient with upd(15)mat; PWS2, a PWS patient with an epimutation (hypermethylation) of the *SNRPN*-DMR; AS1, an Angelman syndrome (AS) patient with upd(15)pat; and AS2, an AS patient with an epimutation (hypomethylation) of the *SNRPN*-DMR.

cell lineage at the very early developmental stage. Hence, in a strict sense, this patient is neither a chimera resulting from the fusion of two different zygotes nor a mosaic caused by a mitotic error of a single zygote. In this regard, a triploid cell stage is assumed in the generation of a upid(AC)mat cell lineage, and such triploid cells may have been detected in skin fibroblasts of the patient reported by Horike *et al*.[3]

The upid(AC)mat cells accounted for the majority of leukocytes even in adulthood of this patient, despite global negative selective pressure.[12 13] This phenomenon, though intriguing, would not be unexpected in human studies because leukocytes are usually utilised for genetic analyses. Rather, if the upid(AC)mat cells were barely present in leukocytes, they would not have been detected. It is likely, therefore, that upid(AC)mat cells have occupied a relatively large portion of the definitive haematopoietic tissues primarily as a stochastic event. Furthermore, parthenogenetic chimera mouse studies have revealed that parthenogenetic cells are found at a relatively high frequency in some tissues/organs including blood and are barely identified in other tissues/organs such as skeletal muscle and liver.[13] Such a possible tissue-specific selection in favour of the preservation of parthenogenetic cells in the definitive haematopoietic tissues may also be relevant to the predominance of the upid(AC)mat cells in leukocytes. In addition, a reduced growth potential of 45,X cells[14] may also have contributed to the skewed ratio of the two cell lineages.

Clinical features of this patient would be determined by several factors. They include: (1) the ratio of two cell lineages in various tissues/organs, (2) the number of imprinted regions or DMRs relevant to the development of specific imprinting disorders (eg, plural regions/DMRs on chromosomes 7 and 11 for SRS[9 10] and a single region/DMR on chromosome 15 for Prader–Willi syndrome (PWS)),[15] (3) the degree of clinical effects of dysregulated imprinted regions/DMRs (an (epi)dominant effect has been

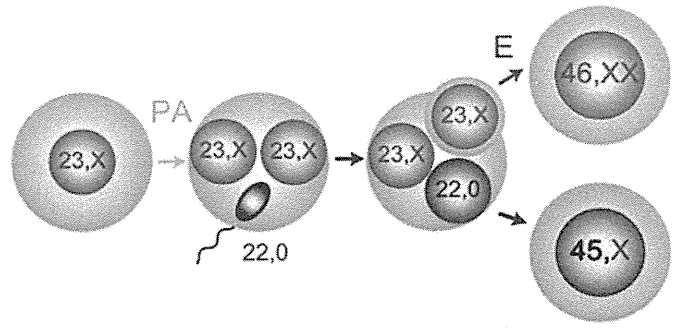

Figure 2 Schematic representation of the generation of the upid(AC)mat 46,XX cell lineage and the non-upd 45,X cell lineage. Polar bodies are not shown. PA, parthenogenetic activation; and E, endoreplication of one blastomere containing a female pronucleus.

J Med Genet 2010;**47**:782–785. doi:10.1136/jmg.2010.079343

assumed for the 11p15.5 imprinted regions including the *IGF2–H19* domain on the basis of SRS or Beckwith–Wiedemann syndrome (BWS) phenotype in patients with multilocus hypomethylation[16] and BWS-like phenotype in patients with a upid (AC)pat cell lineage,[17] a mirror image of a upid(AC)mat cell lineage), (4) expression levels of imprinted genes in upid(AC)mat cells (although *SNRPN* expression of this patient was consistent with upid(AC)mat cells being predominant in leukocytes, complicated expression patterns have been identified for several imprinted genes in androgenetic and parthenogenetic fetal mice, probably because of perturbed *cis*- and *trans*-acting regulatory mechanisms)[18] and (5) unmasking of possible maternally inherited recessive mutation(s) in upid(AC)mat cells.[19] Collectively, it appears that the extent of overall (epi)genetic aberrations exceeded the threshold level for the development of SRS phenotype and horseshoe kidney characteristic of TS[4] but remained below the threshold level for the occurrence of other imprinting disorders or recessive Mendelian disorders.

In summary, we identified a upid(AC)mat 46,XX cell lineage in a woman with an SRS-like phenotype and a 45,X cell lineage accompanied by autosomal haploid sets of biparental origin. This report will facilitate further identification of patients with a upid(AC)mat cell lineage and better clarification of the clinical phenotypes in such patients.

Acknowledgements We thank the patient and her family members for their participation in this study. We also thank Dr. Toshiro Nagai for providing us with blood samples of patients with Prader–Willi syndrome.

Funding This work was supported by grants from the Ministry of Health, Labor, and Welfare and from the Ministry of Education, Science, Sports and Culture.

Competing interests None.

Patient consent Obtained.

Ethics approval This study was conducted with the approval of the Institutional Review Board Committees at National Center for Child health and Development.

Contributors Drs Kazuki Yamazawa (first author) and Kazuhiko Nakabayashi (second author) contributed equally to this work.

Provenance and peer review Not commissioned; externally peer reviewed.

REFERENCES

1. **McGrath J,** Solter D. Completion of mouse embryogenesis requires both the maternal and paternal genomes. *Cell* 1984;**37**:179–83.
2. **Strain L,** Warner JP, Johnston T, Bonthron DT. A human parthenogenetic chimaera. *Nat Genet* 1995;**11**:164–9.
3. **Horike S,** Ferreira JC, Meguro-Horike M, Choufani S, Smith AC, Shuman C, Meschino W, Chitayat D, Zackai E, Scherer SW, Weksberg R. Screening of DNA methylation at the H19 promoter or the distal region of its ICR1 ensures efficient detection of chromosome 11p15 epimutations in Russell–Silver syndrome. *Am J Med Genet Part A* 2009;**149A**:2415–23.
4. **Styne D,** Grumbach M. Puberty: ontogeny, neuroendocrinology, physiology, and disorders. In: Kronenberg H, Melmed M, Polonsky K, Larsen P, eds. *Williams textbook of endocrinology*, 11th edn. Philadelphia: Saunders 2008:969–1166.
5. **Thiede C,** Prange-Krex G, Freiberg-Richter J, Bornhauser M, Ehninger G. Buccal swabs but not mouthwash samples can be used to obtain pretransplant DNA fingerprints from recipients of allogeneic bone marrow transplants. *Bone Marrow Transplant* 2000;**25**:575–7.
6. **Brena RM,** Auer H, Kornacker K, Hackanson B, Raval A, Byrd JC, Plass C. Accurate quantification of DNA methylation using combined bisulfite restriction analysis coupled with the Agilent 2100 Bioanalyzer platform. *Nucleic Acids Res* 2006;**34**:e17.
7. **Yamazawa K,** Kagami M, Nagai T, Kondoh T, Onigata K, Maeyama K, Hasegawa T, Hasegawa Y, Yamazaki T, Mizuno S, Miyoshi Y, Miyagawa S, Horikawa R, Matsuoka K, Ogata T. Molecular and clinical findings and their correlations in Silver–Russell syndrome: implications for a positive role of IGF2 in growth determination and differential imprinting regulation of the IGF2-H19 domain in bodies and placentas. *J Mol Med* 2008;**86**:1171–81.
8. **Yamazawa K,** Kagami M, Ogawa M, Horikawa R, Ogata T. Placental hypoplasia in maternal uniparental disomy for chromosome 7. *Am J Med Genet Part A* 2008;**146A**:514–16.
9. **Abu-Amero S,** Monk D, Frost J, Preece M, Stanier P, Moore GE. The genetic aetiology of Silver–Russell syndrome. *J Med Genet* 2008;**45**:193–9.
10. **Eggermann T,** Eggermann K, Schonherr N. Growth retardation versus overgrowth: Silver–Russell syndrome is genetically opposite to Beckwith–Wiedemann syndrome. *Trends Genet* 2008;**24**:195–204.
11. **Goto T,** Monk M. Regulation of X-chromosome inactivation in development in mice and humans. *Microbiol Mol Biol Rev* 1998;**62**:362–78.
12. **Nagy A,** Sass M, Markkula M. Systematic non-uniform distribution of parthenogenetic cells in adult mouse chimaeras. *Development* 1989;**106**:321–4.
13. **Fundele R,** Norris ML, Barton SC, Reik W, Surani MA. Systematic elimination of parthenogenetic cells in mouse chimeras. *Development* 1989;**106**:29–35.
14. **Verp MS,** Rosinsky B, Le Beau MM, Martin AO, Kaplan R, Wallemark CB, Otano L, Simpson JL. Growth disadvantage of 45, X and 46, X, del(X)(p11) fibroblasts. *Clin Genet* 1988;**33**:277–85.
15. **Horsthemke B,** Wagstaff J. Mechanisms of imprinting of the Prader–Willi/Angelman region. *Am J Med Genet A* 2008;**146A**:2041–52.
16. **Azzi S,** Rossignol S, Steunou V, Sas T, Thibaud N, Danton F, Le Jule M, Heinrichs C, Cabrol S, Gicquel C, Le Bouc Y, Netchine I. Multilocus methylation analysis in a large cohort of 11p15-related foetal growth disorders (Russell Silver and Beckwith Wiedemann syndromes) reveals simultaneous loss of methylation at paternal and maternal imprinted loci. *Hum Mol Genet* 2009;**18**:4724–33.
17. **Wilson M,** Peters G, Bennetts B, McGillivray G, Wu ZH, Poon C, Algar E. The clinical phenotype of mosaicism for genome-wide paternal uniparental disomy: two new reports. *Am J Med Genet Part A* 2008;**146A**:137–48.
18. **Ogawa H,** Wu Q, Komiyama J, Obata Y, Kono T. Disruption of parental-specific expression of imprinted genes in uniparental fetuses. *FEBS Lett* 2006;**580**:5377–84.
19. **Engel E.** A fascination with chromosome rescue in uniparental disomy: Mendelian recessive outlaws and imprinting copyrights infringements. *Eur J Hum Genet* 2006;**14**:1158–69.

RESEARCH LETTER

AMERICAN JOURNAL OF medical genetics

Prenatal Findings of Paternal Uniparental Disomy 14: Delineation of Further Patient

Nobuhiro Suzumori,[1,2]* Tsutomu Ogata,[3] Eita Mizutani,[1,2] Yukio Hattori,[1] Keiko Matsubara,[3] Masayo Kagami,[3] and Mayumi Sugiura-Ogasawara[1]

[1]Department of Obstetrics & Gynecology, Nagoya City University Graduate School of Medicine, Nagoya, Japan

[2]Division of Molecular and Clinical Genetics, Nagoya City University Graduate School of Medicine, Nagoya, Japan

[3]Department of Endocrinology and Metabolism, National Research Institute for Child Health and Development, Tokyo, Japan

Received 5 March 2010; Accepted 2 August 2010

TO THE EDITOR:

Human chromosome 14q32.2 carries a cluster of imprinted genes including paternally expressed genes such as *DLK1* and *RTL1* and maternally expressed genes such as *MEG3* (alias *GTL2*) and *RTL1as* (*RTL1* antisense), together with the germline-derived intergenic differentially methylated region (IG-DMR) and the postfertilization-derived *MEG3*-DMR [da Rocha et al., 2008; Kagami et al., 2008a]. Consistent with this, paternal uniparental disomy 14 (upd(14)pat) results in a unique phenotype characterized by facial abnormality, small bell-shaped thorax with coat-hanger appearance of the ribs, abdominal wall defects, placentomegaly, and polyhydramnios [Kagami et al., 2008a,b], and maternal uniparental disomy 14 (upd(14)mat) leads to less-characteristic but clinically discernible features including growth failure [Kotzot, 2004; Kagami et al., 2008a].

For upd(14)pat, this condition has primarily been identified by the pathognomonic chest roentgenographic findings that are obtained immediately after birth because of severe respiratory dysfunction [Kagami et al., 2008a]. However, upd(14)pat has also been suspected prenatally by fetal radiological findings suggestive of small thorax and other characteristic findings [Curtis et al., 2006; Yamanaka et al., 2010]. Here, we report on prenatal findings in a hitherto unreported upd(14)pat patient. The results will serve to the prenatal identification of similarly affected patients and appropriate neonatal care including respiratory management.

A 41-year-old gravida 1, para 0 Japanese woman was referred to Nagoya City University Hospital because of polyhydramnios at 24 weeks of gestation. The polyhydramnios was severe and required repeated amnioreduction (1,600 ml at 26 weeks, 1,800 ml at 29 weeks, 2,000 ml at 32 weeks, and 2,100 ml at 35 weeks). The fetal urine volume was normal (5–12 ml per hr). At 28 weeks of gestation, 3D ultrasound studies were performed, delineating dysmorphic face, anteverted nares, micrognathia and small thorax characteristic of upd(14)pat (Fig. 1), although the differential diagnosis included Beckwith–Wiedemann syndrome and several types of skeletal dysplasia. Thereafter, ultrasound studies were weekly carried out, indicating almost normal fetal growth and normal umbilical artery Doppler.

How to Cite this Article:
Suzumori N, Ogata T, Mizutani E, Hattori Y, Matsubara K, Kagami M, Sugiura-Ogasawara M. 2010. Prenatal Findings of Paternal Uniparental Disomy 14: Delineation of Further Patient.
Am J Med Genet Part A 152A:3189–3192.

At 37 weeks of gestation, a 2,778 g male infant was delivered by cesarean because of fetal distress. The placenta was 1,384 g (gestational age-matched reference, 510 ± 98 g) [Kagami et al., 2008b]. The patient had severe asphyxia, and immediately received appropriate management including mechanical ventilation for 6 days and nasal directional positive airway pressure at the neonatal intensive care unit. At birth, physical examination revealed hairy forehead, blepharophimosis, depressed nasal bridge, anteverted nares, small ears, protruding philtrum, puckered lips, micrognathia, short webbed neck, joint contractures, and diastasis recti, and roentgenograms showed typical bell-shaped thorax with coat-hanger appearance of the ribs (Fig. 2). Coax valga or kyphoscoliosis was uncertain. Discharge from hospital was 35 days after birth. On the last examination at 8 months of age, the patient

*Correspondence to:
Nobuhiro Suzumori, M.D., Ph.D., Division of Molecular and Clinical Genetics, Department of Obstetrics 8601, Japan.
E-mail: og.n.suz@med.nagoya-cu.ac.jp
Published online 24 November 2010 in Wiley Online Library (wileyonlinelibrary.com)
DOI 10.1002/ajmg.a.33719

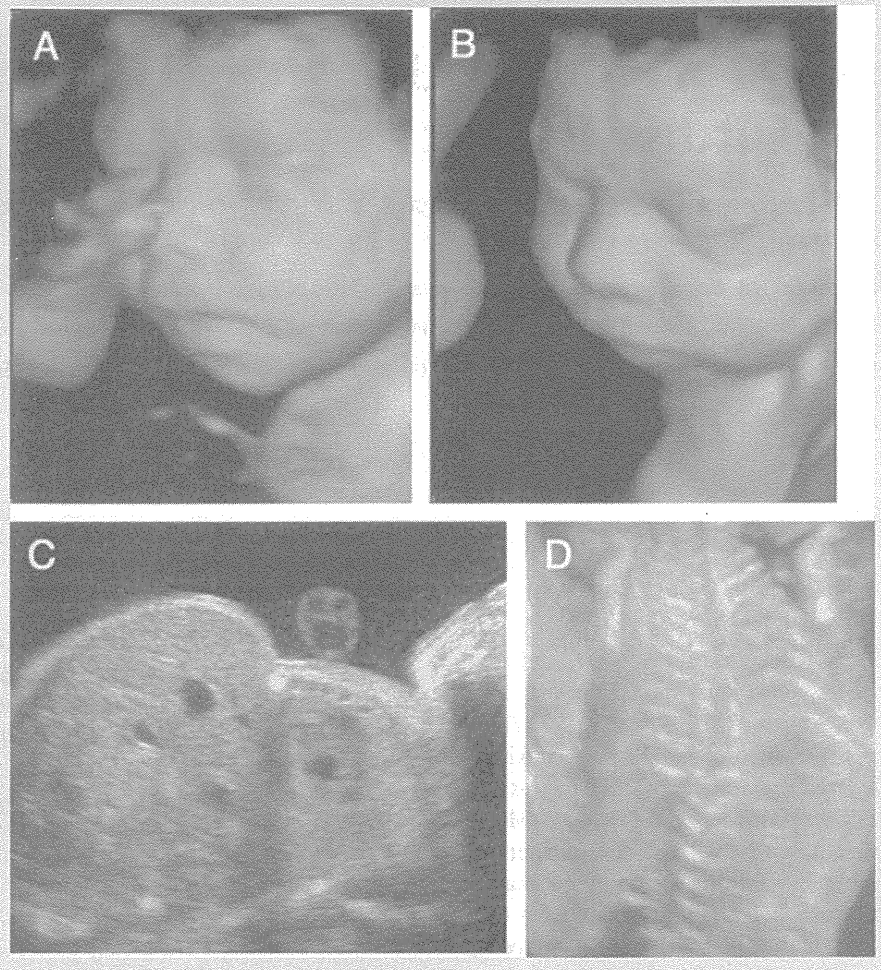

FIG. 1. Prenatal 3D findings at 28 weeks of gestation. A,B: Face appearance with blepharophimosis, depressed nasal bridge, anteverted nares, and micrognathia. C: Small thorax and polyhydramnios. D: Coat-hanger like appearance of the ribs.

required regular oropharyngeal suction and nasogastric tube feeding due to a poor swallowing reflex, and showed developmental delay. At the time of the last evaluation there was no seizure disorder.

To confirm the findings, cytogenetic and molecular studies were performed for the cord blood of the patient by the previously described methods [Kagami et al., 2008a]. This study was approved by the Institutional Review Board Committees at National Center for Child Health and Development and Nagoya City University, and performed after obtaining written informed consent. The karyotype was normal, and metaphase fluorescence in situ hybridization (FISH) analysis with a 202 kb BAC probe containing *DLK1* (RP11-566J3) and a 165 kb BAC probe containing *MG3* and *RTL1/RTL1as* (RP11-123M6) (http://bacpac.-chori.org/) delineated two signals with a similar intensity, respectively. Methylation analysis for bisulfite-treated genomic DNA indicated the presence of paternally derived hypermethylated IG-DMR (CG4 and CG6) and *MEG3*-DMR (CG7) and the absence of maternally derived hypomethylated DMRs. Furthermore, microsatellite analysis was performed using leukocyte genomic DNA of patient and parents, revealing uniparental paternal isodisomy for chromosome 14 (Table I, Fig. 3).

In this patient with molecularly confirmed upd(14)pat, ultrasound studies unequivocally showed typical upd(14)pat phenotypes such as thoracic abnormality and facial dysmorphic features. While this is the first report documenting the facial appearance of the affected fetus, small thorax has been suspected prenatally in five patients with upd(14)pat or epimutations of the IG-DMR and the *MEG3*-DMR, with coat-hanger appearance of the ribs being delineated in one patient [Curtis et al., 2006; Yamanaka et al., 2010]. In this regard, it is notable that polyhydramnios has invariably been identified in upd(14)pat by the second trimester [Kagami et al., 2008a]. It is recommended, therefore, to perform radiological studies for pregnant women with polyhydramnios, to suspect upd(14)pat-compatible clinical features of the fetus. This will permit appropriate counseling and delivery planning at a tertiary

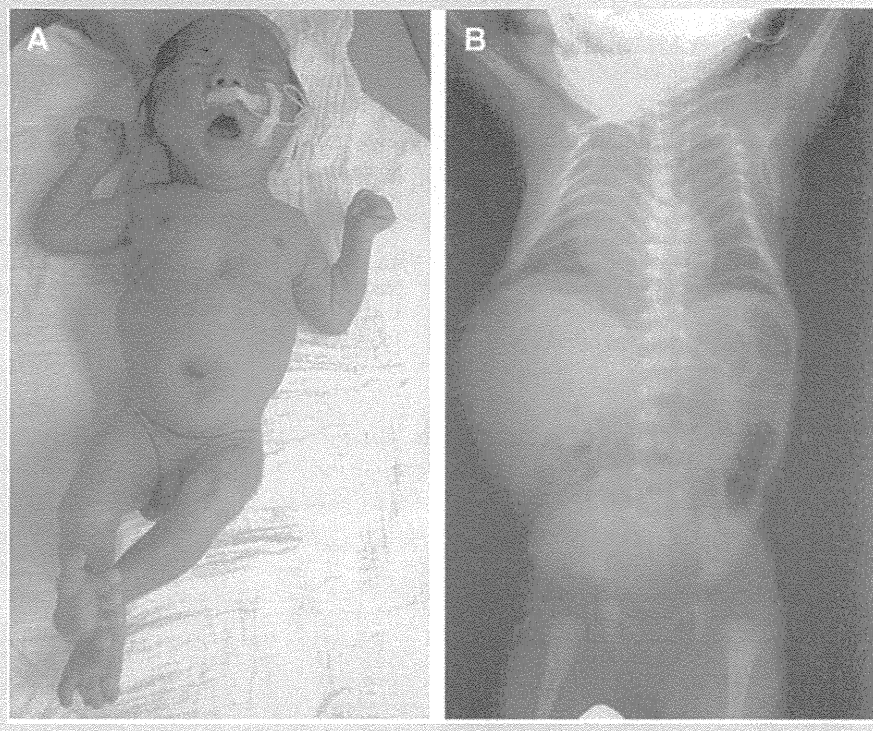

FIG. 2. Postnatal findings at 1 month of age. A: Front view. B: Chest roentgenogram showing bell-shaped thorax with coat-hanger appearance of the ribs.

center with neonatal intensive care as well as pertinent molecular studies using cord blood.

ACKNOWLEDGMENTS

We thank Dr. Saori Kaneko for her assistance in coordinating this research. We also acknowledge the cooperation of the patient's family in allowing us to publish their information.

TABLE I. The Results of Microsatellite Analysis

Locus	Location	Mother	Patient	Father	Assessment
D14S80	14q12	98	98	98	N.I.
D14S608	14q12	200	194	194/210	Isodisomy
D14S588	14q23–24.1	114/126	114	114/122	N.I.
D14S617	14q32.12	139/169	143	143/165	Isodisomy
D14S250	14q32.2	159	159	159/167	N.I.
D14S1006	14q32.2	127/139	127	127/139	N.I.
D14S985	14q32.2	135/137	131	131/133	Isodisomy
D14S1010	14q32.33	134/142	142	142/144	N.I.
D14S1007	14q32.33	119	119	119	N.I.

N.I., not informative.
The Arabic numbers indicate the PCR product sizes in bp.
The imprinted region resides at 14q32.2.
D14S985 is located in the intron of *MEG3*.

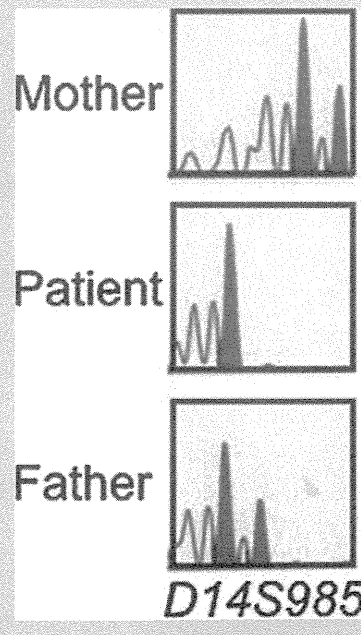

FIG. 3. Microsatellite analysis for *D14S985* residing in the intron of *MEG3*. One of the two peaks in the father is transmitted to the patient, and both of the two peaks in the mother are not inherited by the patient. The PCR fragment size: 135 and 137 bp in the mother, 131 bp in the patient, and 131 and 133 bp in the father. [Color figure can be viewed in the online issue, which is available at wileyonlinelibrary.com]

REFERENCES

Curtis L, Antonelli E, Vial Y, Rimensberger P, Merrer ML, Hinard C, Bottani A, Fokstuen S. 2006. Prenatal diagnostic indicators of paternal uniparental disomy 14. Prenat Diagn 26:662–666.

da Rocha ST, Edwards CA, Ito M, Ogata T, Ferguson-Smith AC. 2008. Genomic imprinting at the mammalian Dlk1-Dio3 domain. Trends Genet 24:306–316.

Kagami M, Sekita Y, Nishimura G, Irie M, Kato F, Okada M, Yamamori S, Kishimoto H, Nakayama M, Tanaka Y, Matsuoka K, Takahashi T, Noguchi M, Tanaka Y, Masumoto K, Utsunomiya T, Kouzan H, Komatsu Y, Ohashi H, Kurosawa K, Kosaki K, Ferguson-Smith AC, Ishino F, Ogata T. 2008a. Deletions and epimutations affecting the human 14q32.2 imprinted region in individuals with paternal and maternal upd(14)-like phenotypes. Nat Genet 40:237–242.

Kagami M, Yamazawa K, Matsubara K, Matsuo N, Ogata T. 2008b. Placentomegaly in paternal uniparental disomy for human chromosome 14. Placenta 29:760–761.

Kotzot D. 2004. Maternal uniparental disomy 14 dissection of the phenotype with respect to rare autosomal recessively inherited traits, trisomy mosaicism, and genomic imprinting. Ann Genet 47: 251–260.

Yamanaka M, Ishikawa H, Saito K, Maruyama Y, Ozawa K, Shibasaki J, Nishimura G, Kurosawa K. 2010. Prenatal findings of paternal uniparental disomy 14: Report of four patients. Am J Med Genet Part A 152A:789–791.

Journal of Human Genetics (2011) 56, 91–93

www.nature.com/jhg

SHORT COMMUNICATION

Androgenetic/biparental mosaicism in a girl with Beckwith–Wiedemann syndrome-like and upd(14)pat-like phenotypes

Kazuki Yamazawa[1,5], Kazuhiko Nakabayashi[2], Kentaro Matsuoka[3], Keiko Masubara[1], Kenichiro Hata[2], Reiko Horikawa[4] and Tsutomu Ogata[1]

This report describes androgenetic/biparental mosaicism in a 4-year-old Japanese girl with Beckwith–Wiedemann syndrome (BWS)-like and paternal uniparental disomy 14 (upd(14)pat)-like phenotypes. We performed methylation analysis for 18 differentially methylated regions on various chromosomes, genome-wide microsatellite analysis for a total of 90 loci and expression analysis of *SNRPN* in leukocytes. Consequently, she was found to have an androgenetic 46,XX cell lineage and a normal 46,XX cell lineage, with the frequency of the androgenetic cells being roughly calculated as 91% in leukocytes, 70% in tongue tissues and 79% in tonsil tissues. It is likely that, after a normal fertilization between an ovum and a sperm, the paternally derived pronucleus alone, but not the maternally derived pronucleus, underwent a mitotic division, resulting both in the generation of the androgenetic cell lineage by endoreplication of one blastomere containing a paternally derived pronucleus and in the formation of the normal cell lineage by union of paternally and maternally derived pronuclei. It appears that the extent of overall (epi)genetic aberrations exceeded the threshold level for the development of BWS-like and upd(14)pat-like phenotypes, but not for the occurrence of other imprinting disorders or recessive Mendelian disorders.
Journal of Human Genetics (2011) **56**, 91–93; doi:10.1038/jhg.2010.142; published online 11 November 2010

Keywords: androgenesis; Beckwith–Wiedemann syndrome; mosaicism; upd(14)pat

INTRODUCTION

A pure androgenetic human with paternal uniparental disomy for all chromosomes is incompatible with life because of genomic imprinting.[1,2] However, a human with an androgenetic cell lineage could be viable in the presence of a normal cell lineage. Indeed, an androgenetic cell lineage has been identified in six liveborn individuals with variable phenotypes.[3–7] All the androgenetic cell lineages have a 46,XX karyotype, and this is consistent with the lethality of an androgenetic 46,YY cell lineage.

Here, we report on a girl with androgenetic/biparental mosaicism, and discuss the underlying factors for the phenotypic development.

CASE REPORT

This patient was conceived naturally to non-consanguineous and healthy parents. At 24 weeks gestation, the mother was referred to us because of threatened premature delivery. Ultrasound studies showed Beckwith–Wiedemann syndrome (BWS)-like features,[8] such as macroglossia, organomegaly and umbilical hernia, together with polyhydramnios and placentomegaly. The mother repeatedly received amnioreduction and tocolysis.

She was delivered by an emergency cesarean section because of preterm rupture of membranes at 34 weeks of gestation. Her birth weight was 3730 g (+4.8 s.d. for gestational age), and her length 45.6 cm (+0.7 s.d.). The placenta weighed 1040 g (+7.3 s.d.).[9] She was admitted to a neonatal intensive care unit due to asphyxia. Physical examination confirmed a BWS-like phenotype. Notably, chest roentgenograms delineated mild bell-shaped thorax characteristic of paternal uniparental disomy 14 (upd(14)pat),[10] although coat hanger appearance of the ribs indicative of upd(14)pat was absent (Supplementary Figure 1). She was placed on mechanical ventilation for 2 months, and received tracheostomy, glossectomy and tonsillectomy in her infancy, due to upper airway obstruction. She also had several clinical features occasionally reported in BWS[8] (Supplementary Table 1). Her karyotype was 46,XX in all the 50 lymphocytes analyzed. On the last examination at 4 years of age, she showed postnatal growth failure and severe developmental retardation.

[1]Department of Molecular Endocrinology, National Research Institute for Child Health and Development, Tokyo, Japan; [2]Department of Maternal-Fetal Biology, National Research Institute for Child Health and Development, Tokyo, Japan; [3]Division of Pathology, National Medical Center for Children and Mothers, Tokyo, Japan and [4]Division of Endocrinology and Metabolism, National Medical Center for Children and Mothers, Tokyo, Japan
[5]Current address: Department of Physiology, Development & Neuroscience, University of Cambridge, Cambridge, UK.
Correspondence: Dr T Ogata, Department of Molecular Endocrinology, National Research Institute for Child Health and Development, 2-10-1 Ohkura, Setagaya, Tokyo 157-8535, Japan.
E-mail: tomogata@nch.go.jp
Received 9 September 2010; revised 18 October 2010; accepted 22 October 2010; published online 11 November 2010

MOLECULAR STUDIES

This study was approved by the Institutional Review Board Committee at the National Center for Child health and Development, and performed after obtaining informed consent.

Methylation analysis

We first performed bisulfite sequencing for the *H19*-DMR (differentially methylated region) and KvDMR1 as a screening of BWS[11,12] and that for the IG-DMR and the *MEG3*-DMR as a screening of upd(14)pat,[10] using leukocyte genomic DNA. Paternally derived clones were predominantly identified for the four DMRs examined (Figure 1a). We next performed combined bisulfite restriction analysis for multiple DMRs, as reported previously.[13] All the autosomal DMRs exhibited markedly skewed methylation patterns consistent with predominance of paternally inherited clones, whereas the *XIST*-DMR on the X chromosome showed a normal methylation pattern (Figure 1a).

Genome-wide microsatellite analysis

Microsatellite analysis was performed for 90 loci with high heterozygosities in the Japanese population.[14] Major peaks consistent with paternal uniparental isodisomy and minor peaks of maternal origin were identified for at least one locus on each chromosome, with the minor peaks of maternal origin being more obvious in tongue and tonsil tissues than in leukocytes (Figure 1b and Supplementary Table 2). There were no loci with three or four peaks indicative of chimerism. The frequency of the androgenetic cells was calculated as 91% in leukocytes, 70% in tongue cells and 79% in tonsil cells, although the estimation apparently was a rough one (for details, see Supplementary Methods).

Expression analysis

We examined *SNRPN* expression, because *SNRPN* showed strong expression in leukocytes (for details, see Supplementary Data). *SNRPN* expression was almost doubled in the leukocytes of this patient (Figure 1c).

DISCUSSION

These results suggest that this patient had an androgenetic 46,XX cell lineage and a normal 46,XX cell lineage. In this regard, both the androgenetic and the biparental cell lineages appear to have derived from a single sperm and a single ovum, because a single haploid genome of paternal origin and that of maternal origin were identified in this patient by genome-wide microsatellite analysis. Thus, it is likely that after a normal fertilization between an ovum and a sperm, the paternally derived pronucleus alone, but not the maternally derived pronucleus, underwent a mitotic division, resulting both in the generation of the androgenetic cell lineage by endoreplication of

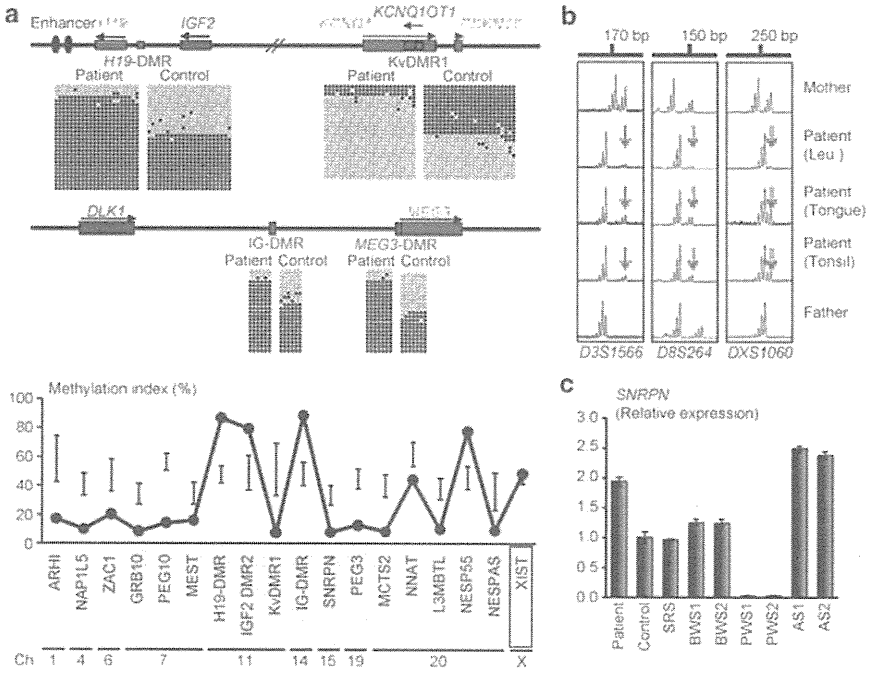

Figure 1 Representative molecular results. (**a**) Methylation analysis. Upper part: Bisulfite sequencing data for the *H19*-DMR and the KvDMR1 on 11p15.5, and those for the IG-DMR and the *MEG3*-DMR on 14q32.2. Each line indicates a single clone, and each circle denotes a CpG dinucleotide; filled and open circles represent methylated and unmethylated cytosines, respectively. Paternally expressed genes are shown in blue, maternally expressed gene in red, and the DMRs in green. The *H19*-DMR, the IG-DMR, and the *MEG3*-DMR are usually methylated after paternal transmission and unmethylated after maternal transmission, whereas the KvDMR1 is usually unmethylated after paternal transmission and methylated after maternal transmission.[10,11] Lower part: Methylation indices (the ratios of methylated clones) obtained from the COBRA analyses for the 18 DMRs. The DMRs highlighted in blue and pink are methylated after paternal and maternal transmissions, respectively. The black vertical bars indicate the reference data (maximum – minimum) in leukocyte genomic DNA of 20 normal control subjects (the *XIST*-DMR data are obtained from 16 control females). (**b**) Representative microsatellite analysis. Major peaks of paternal origin and minor peaks of maternal origin (red arrows) have been identified in this patient. The minor peaks of maternal origin are more obvious in tongue and tonsil tissues than in leukocytes (Leu.). (**c**) Relative expression level (mean ± s.d.) of *SNRPN*. The data are normalized against *TBP*. SRS: an SRS patient with an epimutation (hypomethylation) of the *H19*-DMR; BWS1: a BWS patient with an epimutation (hypermethylation) of the *H19*-DMR; BWS2: a BWS patient with upd(11)pat; PWS1: a Prader-Willi syndrome (PWS) patient with upd(15)mat; PWS2: a PWS patient with an epimutation (hypermethylation) of the *SNRPN*-DMR; AS1: an Angelman syndrome (AS) patient with upd(15)pat; and AS2: an AS patient with an epimutation (hypomethylation) of the *SNRPN*-DMR. The data were obtained using an ABI Prism 7000 Sequence Detection System (Applied Biosystems).

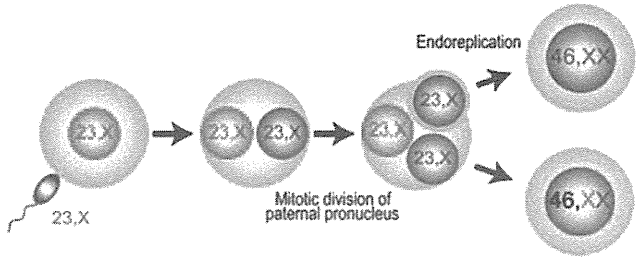

Figure 2 Schematic representation of the generation of the androgenetic/biparental mosaicism. Polar bodies are not shown.

one blastomere containing a paternally derived pronucleus and in the formation of the normal cell lineage by union of paternally and maternally derived pronuclei (Figure 2). This model has been proposed for androgenetic/biparental mosaicism generated after fertilization between a single ovum and a single sperm.[5,15,16] The normal methylation pattern of the *XIST*-DMR is explained by assuming that the two X chromosomes in the androgenetic cell lineage undergo random X-inactivation, as in the normal cell lineage. Furthermore, the results of microsatellite analysis imply that the androgenetic cells were more prevalent in leukocytes than in tongue and tonsil tissues.

A somatic androgenetic cell lineage has been identified in seven liveborn patients including this patient (Supplementary Table 1).[3–7] In this context, leukocytes are preferentially utilized for genetic analyses in human patients, and detailed examinations such as analyses of plural DMRs are necessary to detect an androgenetic cell lineage. Thus, the hitherto identified patients would be limited to those who had androgenetic cells as a predominant cell lineage in leukocytes probably because of a stochastic event and received detailed molecular studies. If so, an androgenetic cell lineage may not be so rare, and could be revealed by detailed analyses as well as examinations of additional tissues in patients with relatively complex phenotypes, as observed in the present patient.

Phenotypic features in androgenetic/biparental mosaicism would be determined by several factors. They include (1) the ratio of two cell lineages in various tissues/organs, (2) the number of imprinted domains relevant to specific features (for example, dysregulation of the imprinted domains on 11p15.5 and 14q32.2 is involved in placentomegaly[9,17]), (3) the degree of clinical effects of dysregulated imprinted domains (an (epi)dominant effect has been assumed for the 11p15.5 imprinted domains[18]), (4) expression levels of imprinted genes in androgenetic cells (although *SNRPN* expression of this patient was consistent with androgenetic cells being predominant in leukocytes, complicated expression patterns have been identified for several imprinted genes in both androgenetic and parthenogenetic fetal mice, probably because of perturbed *cis*- and *trans*-acting regulatory mechanisms[19]) and (5) unmasking of possible paternally inherited recessive mutation(s) in androgenetic cells. Thus, in this patient, it appears that the extent of overall (epi)genetic aberrations exceeded the threshold level for the development of BWS-like and upd(14)pat-like body and placental phenotypes, but remained below the threshold level for the occurrence of other imprinting disorders or recessive Mendelian disorders.

CONFLICT OF INTEREST

The authors declare no conflict of interest.

ACKNOWLEDGEMENTS

This work was supported by grants from the Ministry of Health, Labor, and Welfare, and the Ministry of Education, Science, Sports and Culture.

1 Surani, M. A., Barton, S. C. & Norris, M. L. Development of reconstituted mouse eggs suggests imprinting of the genome during gametogenesis. *Nature* **308,** 548–550 (1984).
2 McGrath, J. & Solter, D. Completion of mouse embryogenesis requires both the maternal and paternal genomes. *Cell* **37,** 179–183 (1984).
3 Hoban, P. R., Heighway, J., White, G. R., Baker, B., Gardner, J., Birch, J. M. *et al.* Genome-wide loss of maternal alleles in a nephrogenic rest and Wilms' tumour from a BWS patient. *Hum. Genet.* **95,** 651–656 (1995).
4 Bryke, C. R., Garber, A. T. & Israel, J. Evolution of a complex phenotype in a unique patient with a paternal uniparental disomy for every chromosome cell line and a normal biparental inheritance cell line. *Am. J. Hum. Genet.* **75**(Suppl), 831 (2004).
5 Giurgea, I., Sanlaville, D., Fournet, J. C., Sempoux, C., Bellanne-Chantelot, C. & Touati, G. Congenital hyperinsulinism and mosaic abnormalities of the ploidy. *J. Med. Genet.* **43,** 248–254 (2006).
6 Wilson, M., Peters, G., Bennetts, B., McGillivray, G., Wu, Z. H., Poon, C. *et al.* The clinical phenotype of mosaicism for genome-wide paternal uniparental disomy: two new reports. *Am. J. Med. Genet. Part A* **146A,** 137–148 (2008).
7 Reed, R. C., Beischel, L., Schoof, J., Johnson, J., Raff, M. L. & Kapur, R. P. Androgenetic/biparental mosaicism in an infant with hepatic mesenchymal hamartoma and placental mesenchymal dysplasia. *Pediatr. Dev. Pathol.* **11,** 377–383 (2008).
8 Jones, K. L. *Smith's Recognizable Patterns of Human Malformation* 6th edn. (Elsevier Saunders: Philadelphia, 2006).
9 Kagami, M., Yamazawa, K., Matsubara, K., Matsuo, N. & Ogata, T. Placentomegaly in paternal uniparental disomy for human chromosome 14. *Placenta* **29,** 760–761 (2008).
10 Kagami, M., Sekita, Y., Nishimura, G., Irie, M., Kato, F., Okada, M. *et al.* Deletions and epimutations affecting the human 14q32.2 imprinted region in individuals with paternal and maternal upd(14)-like phenotypes. *Nat. Genet.* **40,** 237–242 (2008).
11 Yamazawa, K., Kagami, M., Nagai, T., Kondoh, T., Onigata, K., Maeyama, K. *et al.* Molecular and clinical findings and their correlations in Silver-Russell syndrome: implications for a positive role of IGF2 in growth determination and differential imprinting regulation of the IGF2-H19 domain in bodies and placentas. *J. Mol. Med.* **86,** 1171–1181 (2008).
12 Weksberg, R., Shuman, C. & Beckwith, J. B. Beckwith-Wiedemann syndrome. *Eur. J. Hum. Genet.* **18,** 8–14 (2010).
13 Yamazawa, K., Nakabayashi, K., Kagami, M., Sato, T., Saitoh, S., Horikawa, R. *et al.* Parthenogenetic chimaerism/mosaicism with a Silver-Russell syndrome-like phenotype. *J. Med. Genet.* **47,** 782–785 (2010).
14 Ikari, K., Onda, H., Furushima, K., Maeda, S., Harata, S. & Takeda, J. Establishment of an optimized set of 406 microsatellite markers covering the whole genome for the Japanese population. *J. Hum. Genet.* **46,** 207–210 (2001).
15 Kaiser-Rogers, K. A., McFadden, D. E., Livasy, C. A., Dansereau, J., Jiang, R., Knops, J. F. *et al.* Androgenetic/biparental mosaicism causes placental mesenchymal dysplasia. *J. Med. Genet.* **43,** 187–192 (2006).
16 Kotzot, D. Complex and segmental uniparental disomy updated. *J. Med. Genet.* **45,** 545–556 (2008).
17 Monk, D., Arnaud, P., Apostolidou, S., Hills, F. A., Kelsey, G., Stanier, P. *et al.* Limited evolutionary conservation of imprinting in the human placenta. *Proc. Natl. Acad. Sci. USA.* **103,** 6623–6628 (2006).
18 Azzi, S., Rossignol, S., Steunou, V., Sas, T., Thibaud, N., Danton, F. *et al.* Multilocus methylation analysis in a large cohort of 11p15-related foetal growth disorders (Russell Silver and Beckwith Wiedemann syndromes) reveals simultaneous loss of methylation at paternal and maternal imprinted loci. *Hum. Mol. Genet.* **18,** 4724–4733 (2009).
19 Ogawa, H., Wu, Q., Komiyama, J., Obata, Y. & Kono, T. Disruption of parental-specific expression of imprinted genes in uniparental fetuses. *FEBS Lett.* **580,** 5377–5384 (2006).

Supplementary Information accompanies the paper on Journal of Human Genetics website (http://www.nature.com/jhg)